Synthesis of Au(II) Fluoro Complexes and Their Structural and Magnetic Properties

Scott H. Elder, George M. Lucier, Frederick J. Hollander, and Neil Bartlett*

Contribution from the Chemical Sciences Division, Lawrence Berkeley Laboratory, and Department of Chemistry, The University of California at Berkeley, Berkeley, California 94720

Abstract: Gold at ~20 °C with F_2 in anhydrous hydrogen fluoride (aHF) acidified with SbF_5 dissolves to a red solution from which orange $Au^{II}(SbF_6)_2$ crystallizes on removal of volatiles. $Au(SbF_6)_2$ is triclinic with $a = 5.300(1)$ Å, $b = 5.438(1)$ Å, $c = 8.768(2)$ Å, $\alpha = 76.872(3)°$, $\beta = 88.736(3)°$, $\gamma = 68.109(3)°$, $V = 227.79(7)$ Å^3, and $Z = 1$, space group $P\bar{1}$. Each Au(II) atom, at $\bar{1}$, is at the center of an elongated octahedron of F ligands; the four F's of the approximately square AuF_4 unit are at 2.09(2) Å × 2 Å and 2.15(2) Å × 2, each F provided by a different SbF_6 species. The two long Au−F interatomic distances are at 2.64(2) Å. The SbF_6 are grossly distorted in their interactions with the Au. A *cis* pair of F ligands of each SbF_6, make close approach to two different gold atoms, stretching Sb−F to 1.99(2) and 1.94(2) Å. In each case the Sb−F distances *trans* to these stretched Sb−F bonds are short, being 1.85(2) and 1.84(2) Å, respectively. Magnetic susceptibility measurements show antiferromagnetic coupling with a susceptibility decrease below 13 K. Solvolysis of $Au^{II}(SbF_6)_2$ in aHF is accompanied by disproportionation: $4Au(SbF_6)_2 \rightarrow Au + Au_3F_8 + 8SbF_5(solv)$. Fluorination, at ~20 °C, of the solution of $Au(SbF_6)_2$, in SbF_5 acidified aHF, precipitates red crystals of triclinic $Au^{II}\{SbF_6\}_2Au^{II}\{Au^{III}F_4\}_2$ with $a_o = 5.2345(2)$ Å, $b_o = 8.1218(1)$ Å, $c_o = 10.5977(3)$ Å, $\alpha = 100.090(2)°$, $\beta = 100.327(2)°$, $\gamma = 104.877(2)°$, $V = 416.63(2)$ Å^3, space group $P\bar{1}$, and $Z = 1$. It is a simple paramagnet. The structure shows two different Au(II) environments, each approximately square-coordinated by F ligands, one being coordinated *trans* by an F ligand of each of two SbF_6 and similarly by an F ligand from each of two $Au^{III}F_4$ species. The other Au(II) is approximately square-coordinated via bridging F ligands to four different $Au^{III}F_4$ species. $Au^{II}\{SbF_6\}_2Au^{II}\{Au^{III}F_4\}_2$ with $KAuF_4$ in aHF yields Au_3F_8 free of metallic gold, the simple paramagnetism of which indicates the formulation $Au^{II}\{Au^{III}F_4\}_2$.

Introduction

In 1992, Herring *et al.*[1] gave clear ESR and magnetic evidence for Au^{2+}, as a species present in partially reduced $Au(SO_3F)_3$ and as a solvated ion in the strong protonic acid HSO_3F. They reviewed the previous history of Au(II) and pseudo-Au(II) chemistry and pointed out that genuine Au(II) compounds are rare, those known previously appearing to depend[2−4] upon extensive delocalization of the unpaired electron onto the ligands which support that apparent oxidation state. In the study of Herring *et al.*, the hyperfine splitting due to the [197]Au $I = {}^3/_2$ nuclear spin confirmed the essentially Au^{2+} nature of the ESR active species in the very weak Lewis-base environment of SO_3F^-.

In a recent investigation[5] in these laboratories of the room-temperature dissolution of the noble metals in anhydrous hydrogen fluoride (aHF) with F_2 gas as oxidant, it was observed, as had been found previously[6,7] for the BrF_3 solvent system, that solutions made basic with alkali fluoride generally excited a high oxidation state of the noble metal, whereas solutions acidified by strong F^- acceptors (such as SbF_5 or AsF_5) can stabilize a low oxidation state. Thus palladium metal with alkali fluoride, in aHF/F_2, quickly gave $Pd^{IV}F_6{}^{2-}$, whereas in aHF acidified with SbF_5, the final product was $Pd^{II}\{SbF_6\}_2$. *This is*

in harmony with the low electronegativity of a high oxidation state in an anion, because of its electron richness, and with the high electronegativity of that oxidation state in a cation, as a consequence of its electron deficit. By analogy with the palladium system it seemed that a lower oxidation state of gold, than the Au(III) favored by base,[5] might be realizable by dissolution of the metal in aHF acidified with a strong F^- acceptor. Such has proved to be the case.

Gold dissolves, at ~20 °C, with F_2 in aHF acidified with SbF_5, to give a red solution from which orange crystals of $Au^{II}\{SbF_6\}_2$ crystallize. Exhaustive fluorination results in total conversion of the gold to an insoluble crystalline red solid which is $Au^{II}\{SbF_6\}_2Au^{II}\{Au^{III}_4F\}_2$. The crystal structures of these materials and their magnetic properties indicate that they are true Au(II) derivatives. This paper describes these properties and the attempts to prepare AuF_2 by treatment with base in aHF, or by solvolysis, which have resulted in disproportionation to gold, and the mixed-valence fluoride $Au^{II}Au^{III}_2F_8$.

Experimental Section

Materials. F_2 and aHF were used as supplied by Matheson Gas Products, East Rutherford, NH 07073, and SbF_5 as supplied by Ozark Mahoning Inc., Tulsa, OK 74107, the small HF impurity in the latter being of no consequence because of its use in aHF solution. To destroy any water in the aHF it was distilled to any reactor from stock held in a 100 mL capacity FEP tube containing K_2NiF_6 (Ozark Mahoning). Metallic Au, 1.8−2.3 μm powder (99.95%), was used as supplied by Johnson Matthey, Inc., Seabrook, NH 03874.

Apparatus and Technique. All reactors were constructed in T shape from translucent fluorocarbon polymer tubing (FEP) (Chemplast, Inc., Wayne, NJ 07490) joined with Teflon Swagelok compression fittings and equipped with Teflon body valves, having Kel-F stems

[⊗] Abstract published in *Advance ACS Abstracts,* January 15, 1997.
(1) Herring, F. G.; Hwang, G.; Lee, K. C.; Mistry, F.; Phillips, P. S.; Willner, H.; Aubke, F. *J. Am. Chem. Soc.* **1992,** *114,* 1271.
(2) MacCragh, A.; Koski, W. S. *J. Am. Chem. Soc.* **1963,** *85,* 2375; **1965,** *87,* 2496.
(3) Warren, L. F.; Hawthorne, M. F. *J. Am. Chem. Soc.* **1968,** *90,* 4823.
(4) Schlupp, R. L.; Maki, A. H. *Inorg. Chem.* **1974,** *13,* 44.
(5) Lucier, G.; Elder, S. H.; Chacón, L.; Bartlett, N. *Eur. J. Solid State Inorg. Chem.* **1996,** *33,* 809.
(6) Sharpe, A. G. *J. Chem. Soc.* **1953,** 197
(7) Bartlett, N.; Rao, P. R. *Proc. Chem. Soc.* **1964,** 393.

with Teflon tips, as previously described.[8] The typical T-reactor had $1/2$ in. o.d. FEP tubes, heat pressure sealed at one end and drawn down at the open end to $3/8$ in. o.d. to fit a standard $3/8$ in. Swagelok T. A Teflon valve was joined to one end of the crossing to the T, and the reactor was linked to the supply and vacuum line via a $1/4$ in. o.d. FEP tube ∼2 ft long. Each reactor was pretreated with F_2 (to ∼1400 Torr) before it was used. The less volatile reagents (e.g., gold powder together with SbF_5) were placed in the tube at the crossing of the T, in the DRILAB. The aHF was distilled under vacuum to the mixture, at −196 °C, which was then brought to room temperature. As needed, fluorine was added from the supply to a pressure of ∼1400 Torr total pressure (of which ∼760 Torr in the T was due to aHF). (Because of the corrosive effect of acidified aHF on metals, the teflon-valve access to the metal line was opened briefly and only when a 1400 Torr pressure had been established in that line.) The reactor was inclined, so that the crossing arm was nearly horizontal and the other arm nearly vertical. This maximized the F_2−liquid aHF interface and permitted the spreading of the metal along the bottom side of the tube. The mixture, at ∼20 °C, was vigorously agitated by a sideways flicking of the tube by a properly placed rotating arm. As fluorine was consumed (measured intermittently against the 1400 Torr of the supply line) it was replenished periodically. Solutions [of, for example, $Au(SbF_6)_2$] in the aHF were effectively separated from insolubles (e.g., Au) by decantation of the solution to the other arm. In some cases where the insoluble residue was not sensitive to solvolysis by aHF (e.g., Au_3F_8), the aHF was back-distilled from the decanted solution to the reactor limb and cooled to −196 °C, and the thawed aHF was then used to wash the insoluble solid free of aHF-soluble contaminents. This could be repeated as often as necessary. Manipulation of all solids and SbF_5 was carried out in a Vacuum Atmospheres Corp. DRILAB with a dry argon gas atmosphere.

Single Crystal and Powder Containment for X-ray Diffraction. Because of the easy hydrolysis of the gold fluoro complexes, single crystals and powders (packed by quartz ram-rods) were loaded into thin-walled quartz capillaries (Charles Supper Co., 15 Tech Circle, Natick, MA 01760) which had been vacuum dried at 450 °C. Loading techniques were as described[9] for AgF_3. Single crystals were selected and manipulated in the DRILAB, with the aid of a microscope, and to facilitate the secure holding of a crystal, the commercial capillaries were further drawn down and tapered. The capillaries (for both single-crystal and powder) were plugged with KelF grease, removed from the DRILAB, and sealed by drawing down in a small flame.

X-ray Powder Diffraction Photographs (XRDP) were obtained using Ni-filtered Cu Kα radiation using General Electric Co. Precision Cameras (circumference 45 cm, Straumanis loading).

Magnetic Measurements were made using a Superconducting Quantum Interference Device (SQUID) magnetometer as previously described.[10]

Synthesis of $Au(SbF_6)_2$. One arm of a FEP T-reactor was charged with Au (6.8 mmol) and SbF_5 (∼11 mmol) in the DRILAB. With the reactor attached to the vacuum line, aHF (∼5 g) was added to the charge. Fluorine was added to 800 Torr partial pressure in two aliquots, amounting to ∼3.5 mmol, over a 1.5 h period, with vigorous agitation of the tube contents, at ∼20 °C. An intense raspberry-red solution was produced, and fluorination was halted at the first sign of red $Au(SbF_6)_2Au(AuF_4)_2$ crystals, the clear red solution then being decanted into the other leg of the reactor and the volatiles removed under vacuum to give golden-yellow, crystalline $Au(SbF_6)_2$ (1.5 mmol). The remaining aHF-insoluble residue was mainly metallic Au, with some $Au(SbF_6)_2Au(AuF_4)_2$.

Magnetic Susceptibility for $Au(SbF_6)_2$. The magnetic susceptibility of $Au(SbF_6)_2$ exhibited an unexpected antiferromagnetic departure from Curie law behavior, with a Neél temperature of ∼13 K, as indicated in Figure 1.
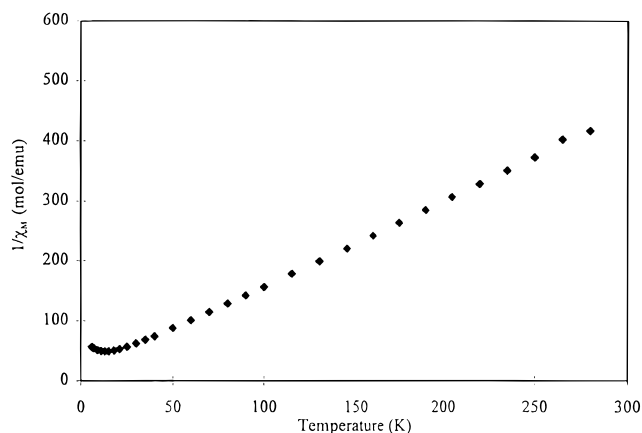

Figure 1. Reciprocal of molar susceptibility (at 5 kG) versus temperature for $Au(SbF_6)_2$; μ_{eff} (for 50−280 K) = $2.37\mu_B$.

The X-ray Single-Crystal Structure of $Au(SbF_6)_2$. The crystal used in the data collection is described in Table SI (Supporting Information), where other pertinent data are also given.

Structural Solution and Refinement. The structure was solved by analysis of similar structures[11,12] and expanded using Fourier maps. All atoms were refined anisotropically. The final cycle of full-matrix least-squares refinement[13] was based on 555 observed reflections ($I > 3.00\sigma(I)$) and 70 variable parameters and converged (largest parameter shift was 0.00 times its esd) with unweighted and weighted agreement factors of

$$R = \sum ||F_o| - |F_c||/\Sigma|F_o| = 0.057$$

$$R_w = \{(\sum w(|F_o| - |F_c|)^2/\Sigma wF_o^2)\}^{1/2} = 0.065$$

The goodness of fit indicator[14] was 2.70. The weighting scheme was based on counting statistics and included a factor ($p = 0.032$) to downweight the intense reflections. Plots of $\sum w(|F_o| - |F_c|)^2$ versus $|F_o|$, reflection order in data collection, $\sin \theta/\lambda$, and various classes of indices, showed no unusual trends. The maximum and minimum peaks on the final difference Fourier map corresponded to 1.53 and −2.87 $e^-/Å^3$, respectively.

Neutral atom scattering factors were taken from Cromer and Waber.[15] Anomalous dispersion effects[16] were included in F_c, and the values for $\Delta f'$ and $\Delta f''$ were those of Creagh and McAuley.[17] The values for the mass attenuation coefficient are those of Creagh and Hubbel.[18] All calculations were performed using the teXsan[19] crystallographic software package of Molecular Structure Corp. Final unit cell parameters are in Table 1, atomic coordinates in Table SII, and anisotropic displacement parameters are in Table SIII. Interatomic distances and angles are in Table SIV.

Solvolysis of $Au(SbF_6)_2$ in aHF. Addition of aHF to solid $Au(SbF_6)_2$ at ∼20 °C rapidly produced a dark brown solid and a pale

(8) Žemva, B.; Hagiwara, R.; Casteel, W. J., Jr.; Lutar, K.; Jesih, A.; Bartlett, N. *J. Am. Chem. Soc.* **1990**, *112*, 4846.

(9) Žemva, B.; Lutar, K.; Jesih, A.; Casteel, W. J., Jr.; Wilkinson, A. P.; Cox, D. E.; Von Dreele, R. B.; Borrmann, H.; Bartlett, N. *J. Am. Chem. Soc.* **1991**, *113*, 4192.

(10) Casteel, W. J., Jr.; Lucier, G.; Hagiwara, R.; Borrmann, H.; Bartlett, N. *J. Solid State Chem.* **1992**, *96*, 84.

(11) Gantar, D.; Leban, I.; Frlec, B.; Holloway, J. H. *J. Chem. Soc., Dalton Trans.* **1987**, 2379.

(12) Lucier, G.; Münzenberg, J.; Casteel, W. J., Jr.; Bartlett, N. *Inorg. Chem.* **1995**, *34*, 2692.

(13) Least-squares function minimized: $\sum w(|F_o| - |F_c|)^2$, where $w = 1/\sigma^2(F_o) = 4F_o^2/\sigma^2(F_o^2)$.

(14) Standard deviation of an observation of unit weight: $[\sum w(|F_o| - |F_c|)^2/(N_o - N_v)]^{1/2}$, where N_o = number of observations and N_v = number of variables.

(15) Cromer, D. T.; Waber, J. T. *International Tables for X-ray Crystallography*; The Kynoch Press: Birmingham, England, 1974; Vol. IV, Table 2.2 A.

(16) Ibers, J. A.; Hamilton, W. C. *Acta Crystallogr.* **1964**, *17*, 781.

(17) Creagh, D. C.; McAuley, W. J. *International Tables for Crystallography*; Wilson, A. J. C., Ed.; Kluwer Academic Publishers: Boston, MA, 1992; Vol. C, Table 4.2.6.8, pp 219−222.

(18) Creagh, D. C.; Hubbell, J. H. *International Tables for Crystallography*; Wilson, A. J. C., Ed.; Kluwer Academic Publishers: Boston, MA, 1992; Vol. C, Table 4.2.4.3, pp 200−206.

(19) teX*san*: Crystal Structure Analysis Package, Molecular Structure Corp. (1985 and 1992).

Table 1. Crystallographic Data for $Au(SbF_6)_2$ and $Au(SbF_6)_2Au(AuF_4)_2$

empirical formula	$AuSb_2F_{12}$	$Au_4Sb_2F_{20}$
formula weight	668.45	1411.34
no. of reflns used for unit cell determn (2θ range)	686 (3.0–45.0°)	1780 (3.0–45.0°)
lattice params		
a (Å)	5.300(1)	5.2345(2)
b (Å)	5.438(1)	8.1218(1)
c (Å)	8.768(2)	10.5977(3)
α (deg)	76.872(3)	100.090(2)
β (deg)	88.736(3)	100.327(2)
γ (deg)	68.109(3)	104.877(2)
V (Å³)	227.79(7)	416.63(2)
space group	$P\bar{1}$ (no. 2)	
Z	1	
D_{calcd} (g/cm³)	4.872	5.625
$F(000)$	289.00	1196.00
μ(Mo Kα) (cm⁻¹)	221.55	385.87
radiation	Mo Kα ($\lambda = 0.710\,69$ Å) graphite monochromated	
temp (K)	296	
residuals: R, R_w, R_{all}	0.057, 0.065, 0.075	0.049, 0.069, 0.050
goodness of fit indicator	2.70	3.11
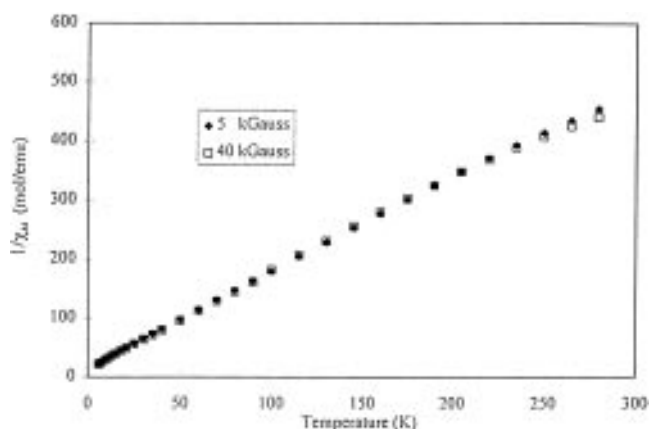
Figure 2. Reciprocal of molar susceptibility (♦, 5 kG; □, 40 kG) versus temperature for $Au(SbF_6)_2Au(AuF_4)_2$; $\mu_{eff} = 2.24\ \mu_B$.

pink solution. Decantation of the pale pink solution [of $Au(SbF_6)_2$ in SbF_5-rich aHF] left a brown solid insoluble in aHF.

$Au(SbF_6)_2$ in aHF with 2KF. KF (0.2 mmol) in aHF (~5 g) was added to $Au(SbF_6)_2$ (0.1 mmol) to produce a dark brown solid from which a colorless solution containing $KSbF_6$ was decanted. The insoluble brown solid was washed five times with back-distilled aHF. XRDP indicated that the insoluble solid was structurally related[10] to $Ag(AuF_4)_2$. The XRDP also contained the pattern of elemental gold, the lines being faint and broad. The soluble product was $KSbF_6$.

Synthesis of $Au(SbF_6)_2Au(AuF_4)_2$. The experimental arrangement for the synthesis of this compound was the same as in the synthesis of $Au(SbF_6)_2$, with the difference that more fluorine was added and the fluorination continued until the supernatant solution was almost colorless. With Au (5.7 mmol) and SbF_5 (10 mmol) in aHF (~5 g), F_2 was added to the reactor in 8 aliquots over a 5 h period, amounting to 8 mmol, which was agitated for a total of 21 h at ~20 °C. The red, highly crystalline $Au(SbF_6)_2Au(AuF_4)_2$ (2.7 mmol, 95% yield) was freed of any soluble products by decantation of the supernatant solution and by one wash with aHF (~5 g).

Magnetic Susceptibility for $Au(SbF_6)_2Au(AuF_4)_2$. The magnetic susceptibility of this solid obeyed the Curie law as shown in Figure 2.

The X-ray Crystal Structure of $Au(SbF_6)_2Au(AuF_4)_2$. The crystal used in the data collection is described in Table SIV, where other pertinent data are also given.

Structure Solution and Refinement. The structure was solved by direct methods.[20] Information on the collection of data and the refinement are given in Table SV. All atoms were refined anisotropically. A correction for secondary extinction was applied (coefficient

$= 2.8(3) \times 10^{-6}$) in the final cycles of least-squares. The final cycle of full-matrix least-squares refinement[13] was based on 1306 observed reflections ($I > 3.00\sigma(I)$) and 122 variable parameters. Agreement factors are given in Table 1. The weighting scheme was based on counting statistics and included a factor ($p = 0.031$) to downweight the intense reflections. Plots of $\sum w(|F_o| - |F_c|)^2$ versus $|F_o|$, reflection order in data collection, $\sin\theta/\lambda$, and various classes of indices showed no unusual trends. The maximum and minimum peaks on the final difference Fourier map corresponded to 2.86 and -2.64 e⁻/Å³, respectively. Neutral atom scattering factors, anomalous dispersion effects, values for $\Delta f'$ and $\Delta f''$, and mass attenuation coefficients were obtained as for the $Au(SbF_6)_2$ structure. All calculations used the same software package. Final unit cell parameters are in Table 1, atomic coordinates in Table SVI, and anisotropic displacement parameters in Table SVII. Interatomic distances and angles are given in Table SVIII.

$Au(SbF_6)_2Au(AuF_4)_2$ with LiF in aHF. LiF (0.58 mmol) in aHF (~3 g) was added to $Au(SbF_6)_2Au(AuF_4)_2$ (0.29 mmol) at ~20 °C and the mixture agitated for ~20 h to ensure complete interaction of the large-particle gold compound with the solution. An insoluble brown sediment was produced beneath a colorless solution. The latter was decanted, the insoluble solid was washed four times with back-distilled aHF, and all volatiles were removed. XRDP showed the soluble product to be $LiSbF_6$ with $LiAuF_4$ and the brown solid to be like[10] $Ag(AuF_4)_2$. Similar treatment of $Au(SbF_6)_2Au(AuF_4)_2$ with a 10-fold molar excess of LiF in aHF produced an insoluble residue of gold and a mixture of $LiAuF_4$ and $LiSbF_6$ from the aHF solution and washings.

Conversion of $Au(SbF_6)_2Au(AuF_4)_2$ to Au_3F_8. One arm of a FEP T-reactor was charged with $Au(SbF_6)_2Au(AuF_4)_2$ and $KAuF_4$ with the latter in greater than 3-fold molar excess. Addition of aHF dissolved the $KAuF_4$ but not the $Au(SbF_6)_2Au(AuF_4)_2$. Prolonged agitation of the mixture converted the red macrocrystalline solid to a golden yellow solid. The solution containing excess $KAuF_4$ was decanted from the solid which was washed once with aHF. XRDP of the yellow solid indicated a close structural relationship[10] with $Ag(AuF_4)_2$ and[9] $Ag(AgF_4)_2$. The diffraction data for Ag_3F_8, $AgAu_2F_8$, and Au_3F_8 are given in Tables SIX, X, and XI. The XRDP of all Au_3F_8 preparations, whether containing metallic gold or not, had the dark background typical of XRDP of poorly crystalline material, and only the stronger lines of the diffraction pattern were observed. This pattern, however, roughly matched the stronger line pattern of $AgAu_2F_8$ in relative line intensities (see Tables SX and SXI). The most complete pattern of the set, was that of Ag_3F_8 (see Table SIX). Each of these patterns has been indexed on the basis of a hexagonal unit cell containing nine formula units. Although this indexing should be regarded as tentative the formula unit volume for each of Ag_3F_8 and $AgAu_2F_8$ is within 2 Å³ of the formula unit volume (FUV) obtained by the sum FUV(AgF_2) + 2[FUV(AF_3)]. The hexagonal unit cells are Ag_3F_8, $a_o = 12.79(1)$, $c_o = 9.95(1)$ Å; $AgAu_2F_8$, $a_o = 12.92(1)$, $c_o = 10.43(1)$ Å; Au_3F_8, $a_o = 12.90(2)$, $c_o = 10.81(2)$ Å. The weight balances for two independent preparations are in accord with the composition Au_3F_8 for the golden-yellow solid and XRDP established the presence of both $KSbF_6$ and $KAuF_4$ in the aHF-soluble products, consistent with the overall reaction.

$$Au(SbF_6)_2Au(AuF_4)_2 + 2KAuF_4 \rightarrow 2Au_3F_8 + 2KSbF_6 \quad (1)$$

In reaction *a*, 61.8 mg of $Au(SbF_6)_2Au(AuF_4)_2$ (0.0438 mmol) treated with 54.5 mg of $KAuF_4$ (0.175 mmol) in aHF (~3 g) gave 65.3 mg of Au_3F_8 and 53.3 mg of $KAuF_4$ with $KSbF_6$. Equation l requires 65.1 mg of Au_3F_8 (0.0876 mmol) and 27.3 mg of $KAuF_4$ (0.0874 mmol) with 24.1 mg of $KSbF_5$ (0.0876 mmol), total 51.4 mg. In *b*, 52.2 mg of $Au(SbF_6)_2Au(AuF_4)_2$ (0.037 mmol) with 38.1 mg of $KAuF_4$ (0.122 mmol) in aHF (~10 g) gave 59.5 mg of Au_3F_8 and 39.8 mg of $KAuF_4$ with $KSbF_6$. Equation 1 requires 55.0 mg of Au_3F_8 (0.074 mmol) and 15.0 mg of $KAuF_4$ (0.048 mmol) with 20.3 mg of $KSbF_6$ (0.074 mmol), total 35.3 mg. The **magnetic susceptibility** of the sample of Au_3F_8 prepared in *a* obeyed the Curie law as shown in Figure 3.

(20) *SIR*92: Altamare, A.; Burla, M. C.; Camalli, M.; Cascarano, M.; Giacovazzo, C.; Guagliardi, A.; Polidori, G. *J. Appl. Crystallogr.*, manuscript in preparation.
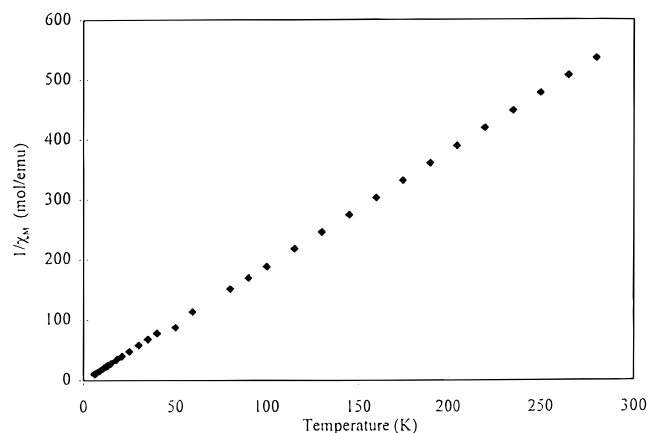
Figure 3. Reciprocal of molar susceptibility (at 5 kG) versus temperature for Au(AuF$_4$)$_2$; $\mu_{\text{eff}} = 2.05$ μ_{B}.
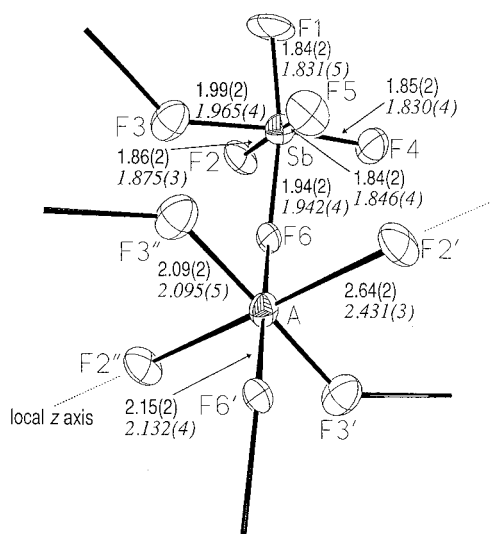

Figure 4. Comparison of bonded-atom interatomic distances (Å) for Au(SbF$_6$)$_2$ and Ag(SbF$_6$)$_2$, values for the latter in italics.

Results and Discussion

Au(SbF$_6$)$_2$ is isostructural with Ag(SbF$_6$)$_2$, which was first prepared and described by Gantar *et al.*[11,21] Figure 4 compares the interatomic distances for the two compounds. In both compounds, the noble-metal atom is at the center of an elongated octahedron of F ligands, each of which is provided by a different SbF$_6$ species. The AF$_6$ distortion (first-order Jahn–Teller) is attributable to the greater antibonding effect of a pair of electrons located in the sigma antibonding orbital (σ^*) designated d$_{z^2}$ (elongation axis z) compared with the single antibonding electron in the σ^* orbital d$_{x^2-y^2}$. Indeed, it is evident from the gross distortion of the SbF$_6^-$ in each of these structures that the Au(II) or Ag(II) atom [A(II)] strongly attracts the F ligands of the four SbF$_6$ species associated with the xy plane of the A(II). It can be seen that the A(II) centers are withdrawing F$^-$ from the SbF$_6^-$, which is one of the poorest F$^-$ donors known.[22,23] The weaker F$^-$ acceptor AsF$_5$, in aHF, is not able to bring about the oxidation of Au to Au(II). Nor is AsF$_5$ able to stabilize Ag(AsF$_6$)$_2$, since systems of that composition in aHF lose AsF$_5$ on crystallization to yield[11,21] the F$^-$ bridged chain-cation salt (AgF)$^{n+}_n$(AsF$_6^-$)$_n$, and only the poorest F$^-$ donor anions (MF$_6$)$^-$ have proved[12] to be capable of stabilizing

Ag(MF$_6$)$_2$. The evident, powerful F$^-$-attracting ability of the A(II) cations must derive from high effective nuclear charge, in spite of these d^9 species having only one electron hole in the valence d shell. The F-ligand arrangements about the two A(II) species, illustrated in Figure 4, show close similarity in the xy plane, but differ appreciably in the local z axis direction.

Since the Au–F and Ag–F distances of the xy plane differ by no more than one ESD, the effective size of the A(II) must be essentially the same in this plane. This must be an accident of cancelling opposing effects. In the metals, the effective size of the gold atom, measured by the formula unit volume of the cubic close packed structure,[24] is slightly less than that of the metallic silver atom (16.97 versus 17.05 Å^3). This derives from a combination of the lanthanide contraction and the impact of the relativistic effect.[25,26] As a consequence of the latter, the atomization enthalpy[27] of gold is greater than that of silver [ΔH_f°(A$_{(g)}$): A = Au, 87.5; A = Ag, 68 kcal mol^{-1}]. This is because, in the higher nuclear-charge gold atom, the binding of the s orbital electrons is enhanced, and the valence electron for the metallic bonding has this character. The slightly smaller metal-atom size of gold relative to silver must, in some measure, represent this greater bonding energy for gold. The separated gaseous atoms should not have the same relative size as in the metal. In the simple A(III) systems the relative sizes are reversed. Thus, in the {A^{III}F$_4$}$^-$ ions, the Au–F interatomic distance is slightly larger[28] than the Ag–F one[29] [Au–F, 1.915(3); Ag–F, 1.889(3) Å], and the same holds for the close set of four F ligands (approximately square planar) in the trifluorides,[9] although the difference there is not significant. This switch in relative size from A(0) to A(III) is in harmony with the involvement of valence d electrons of A in the A(III) fluorospecies bonding. The enhancement of the binding of gold s electrons, destabilizes the d electrons of gold relative to their silver counterparts. Thus, although the valence s electron of the gold [via the a$_{1g}$ orbital of the D_{4h} symmetry (AuF$_4$)$^-$ ion] provides enhanced binding relative to the situation in the silver analogue, the d orbitals of the Au atoms provide less binding energy benefit than in the case of silver. The adverse effects on the binding in AuF$_4^-$ appear to outweigh the benefit derived from the tighter binding of the a$_{1g}$ bonding electron pair. But A(II) in the A(SbF$_6$)$_2$ compounds has an antibonding electron to be associated with the plane (xy) containing the four close ligands. This should weaken the Au(II)–F bonding more than that of Ag(II)–F and enhance the difference already noted for the A(III)–F interatomic distances. Because of the lower precision realized in the Au(SbF$_6$)$_2$ structure, the xy plane Au–F and Ag–F distances are not significantly distinguished from one another. It is possible however that Au^{II}F could be as much as 0.07 Å longer than Ag^{II}F, but not more. The single σ^* electron (identified loosely with the d$_{x^2-y^2}$ orbital) therefore does not appear to have a large impact on the ligand geometry. This is not so for the d$_{z^2}$ electron pair.

The difference of ~0.21 Å in the Au–F and Ag–F distances along the z axis expresses the highly antibonding influence of the d$_{z^2}$ electron pair in the case of Au(II). This and the ~8 Å^3 greater formula unit volume of Au(SbF$_6$)$_2$ (227.8 Å^3) versus

(21) Gantar, D.; Frlec, B.; Russell, D. R.; Holloway, J. H. *Acta Crystallogr.* **1987**, *99*, 685.

(22) Mallouk, T. E.; Rosenthal, G. L.; Müller, G.; Brusasco, R.; Bartlett, N. *Inorg. Chem.* **1984**, *23*, 3167.

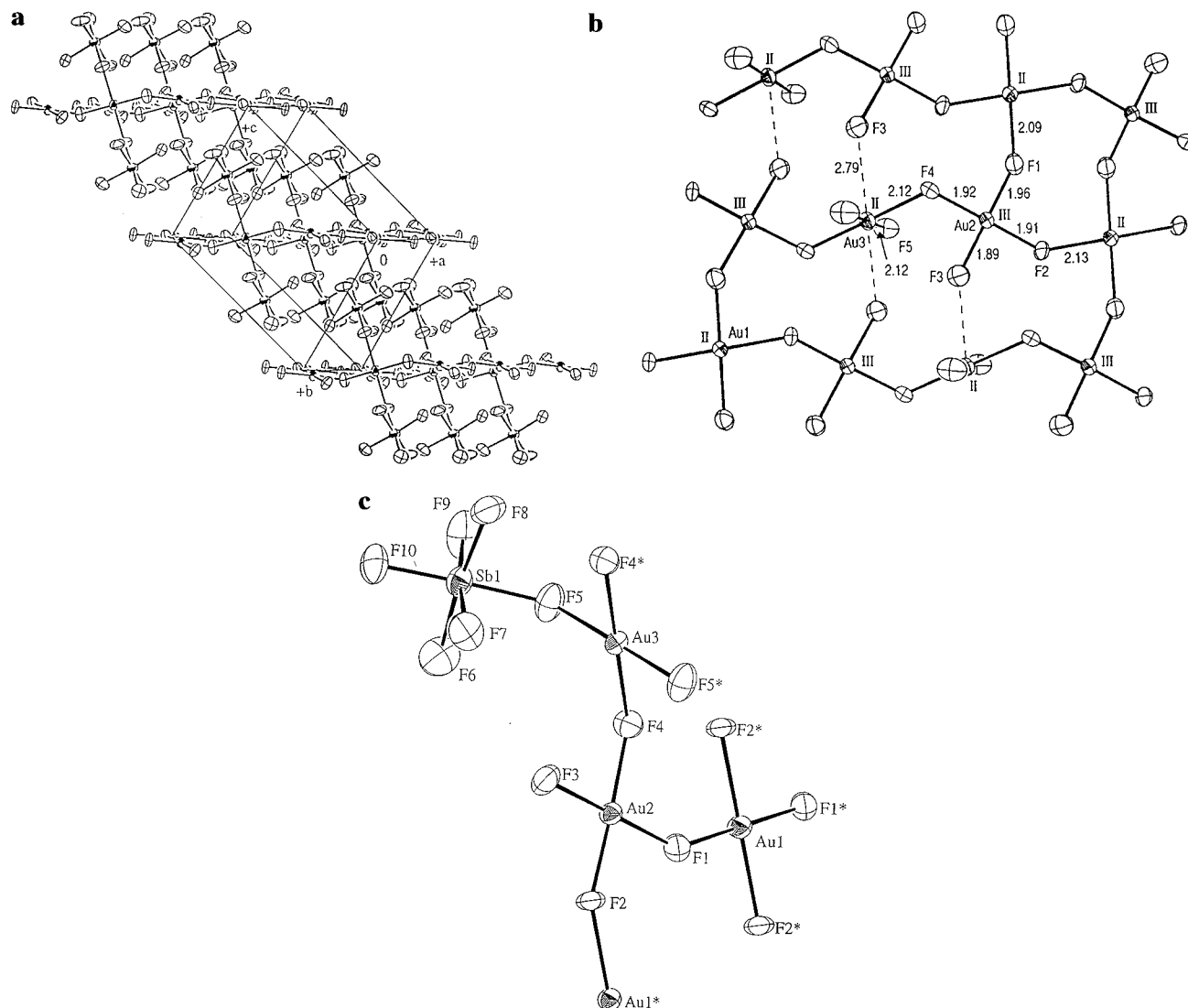(23) Christe, K. O.; Dixon, D. A. *J. Am. Chem. Soc.* **1992**, *114*, 2978.

(24) Wyckoff, R. W. G. *Crystal Structures*; Interscience Publishers: London and Sydney, 1963; Vol. 1.

(25) Pitzer, K. *Acc. Chem. Res.* **1979**, *12*, 271.

(26) Pyykko, P.; Desclaux, J. P. *Acc. Chem. Res.* **1979**, *12*, 276.

(27) NBS Technical Note 270-4, U.S. Department of Commerce, National Bureau of Standards, 1969.

(28) Engelmann, U.; Müller, B. G. *Z. Anorg. Allg. Chem.* **1991**, *598/9*, 103.

(29) Lutar, K.; Milićev, S.; Žemva, B.; Müller, B. G. Bachmann, B.; Hoppe, R. *Eur. J. Solid State Inorg. Chem.* **1991**, *28*, 1335.

a

b

c

Figure 5. Structural features of Au^{II}(SbF$_6$)$_2$Au^{II}{Au^{III}F$_4$}$_2$: (a) sheets of composition AuF$_2$, with sandwiched SbF$_6$; (b) interatomic distances (Å), $\sigma \approx 0.01$ Å, for the AuF$_2$ composition sheet; Roman numerals indicate oxidation states; (c) labeling for the structural unit.

Ag(SbF$_6$)$_2$ (219.7 Å^3) shows that the Au(II) d$_{z^2}$ electron pair has greater effective size than its Ag(II) counterpart. This is similar to Au(III) versus Ag(III) in the trifluorides.[9] It is also in harmony with the ease of addition[30,31] of F$_2$ to the low-spin d^8 configuration of Au(III) in AuF$_4^-$ in its oxidation to Au^{V}F$_6$- and the failure to similarly oxidize Ag(III).

Even though extensive oxidation of gold by F$_2$, in strongly acidified aHF, to Au(SbF$_6$)$_2$ occurs easily, prolonged exposure of the solution of this highly soluble salt to F$_2$ does produce an insoluble further oxidation product. Because of its slow formation and its very low solubility in aHF, the red product is highly crystalline and the X-ray single-crystal structure, represented in Figure 5, shows it to be Au^{II}{SbF$_6$}$_2$Au^{II}{Au^{III}F$_4$}$_2$. The low solubility of the material can be attributed to the polymeric sheet component of the structure, which has the overall composition AuF$_2$. As Figure 5 shows, this sheet involves two different Au(II) species, each at a center of symmetry, $\bar{1}$. One is linked in a square array of four F ligands shared with four separate square Au^{III}F$_4$ units, the other joined to two different Au^{III}F$_4$ groups and to two SbF$_6$ groups, the

latter pendant above and below the AuF$_2$ composition sheet. The SbF$_6$ groups are sandwiched between the AuF$_2$ composition sheets, filling the available space between them, the entire arrangement being a highly close-packed one, the sheets puckering slightly to help make it so.

Justification for these Au oxidation-state assignments is as follows: Each Au atom is approximately square-coordinated by four F ligands, but the three AuF$_4$ species are not chemically equivalent. The longer Au–F interatomic distances of ~2.1 Å, associated with Au1 and Au3, point to these being Au(II) species. The interatomic distances for the bridging F ligands close to Au2, with Au–F ranging from 1.91(1) to 1.96(1) Å are slightly shorter than comparable bonds in AuF$_3$, where[9] two F ligands (of the approximately square array) bridge equally two gold atoms, and have Au–F = 1.998(2) Å. The one nonbridging F ligand associated with Au2 at Au–F = 1.890(9) Å is not significantly different from the "nonbridging" distances of the square ligand arrangement of AuF$_3$, where Au–F = 1.876(3) Å. It is therefore appropriate to assign Au2 as Au(III).

The Curie law paramagnetism of the Au(SbF$_6$)$_2$Au(AuF$_4$)$_2$ displayed in Figure 2 establishes that the Au(II) centers cannot share a common bridging F ligand since that[32] would be associated with strong antiferromagnetic coupling of the Au(II)

(30) Leary, K.; Bartlett, N. *J. Chem. Soc., Chem. Commun.* **1972**, 903. Leary, K.; Zalkin, A.; Bartlett, N. *Inorg. Chem.* **1974**, *13*, 775. Bartlett, N.; Leary, K. *Rev. Chim. Miner.* **1976**, *13*, 82.
(31) Lutar, K.; Jesih, A.; Leban, I.; Žemva, B.; Bartlett, N. *Inorg. Chem.* **1989**, *28*, 3467.

(32) Goodenough, J. B. *Magnetism and the Chemical Bond*; Wiley-Interscience: New York, 1963; p 170.

unpaired electrons. The oxidation-state designation indicated by the crystal structure is therefore in harmony with the magnetic properties, for which the formulation $Au^{II}\{SbF_6\}_2Au^{II}\{Au^{III}F_4\}_2$ is apt.

If, by subtle reduction, the AuF_2 composition sheets of the $Au(SbF_6)_2Au(AuF_4)_2$ structure were freed of their pendant SbF_6 groups, the nonbridging F ligands (F3) of the Au2 AuF_4 groups could then make closer approach to Au3 (making two Au3−F3 connections, indicated by the broken lines in Figure 5b) to complete its four coordination, *intra* sheet. The result would be a puckered sheet of the kind found in AgF_2, as recently described by Hoppe and his co-workers.[33]

The attempted preparation of AuF_2, by addition, at ∼20 °C, of an alkali fluoride solution in aHF to $Au(SbF_6)_2$, in 2:1 molar ratio, rapidly produced a light brown solid insoluble in aHF, from which $KSbF_6$ was removed by its dissolution in the aHF. XRDP showed that the brown solid contained some metallic gold, but the dominant pattern resembled that[9] of $Ag(AgF_4)_2$ and was particularly close to the pattern[10] of $Ag(AuF_4)_2$. [Both $Ag(AgF_4)_2$ and $Ag(AuF_4)_2$ had been previously prepared[9,10] in these laboratories by precipitation from aHF by mixing a soluble Ag^{2+} salt with twice the molar quantity of a soluble $(AF_4)^-$ salt.] This indicated that the mixed oxidation state material $Au^{II}\{Au^{III}F_4\}_2$ had probably been produced, the overall reaction being

$$4Au(SbF_6)_2 + 8KF \rightarrow Au + Au(AuF_4)_2 + 8KSbF_6 \quad (2)$$
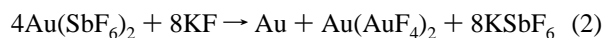
Even the solvolysis of $Au(SbF_6)_2$ by aHF gave the same insoluble brown solid mixture of gold and the conjectured $Au(AuF_4)_2$. Firmer support for that formulation came, however, with the preparation of the $Au(AuF_4)_2$, by metathetical interaction of $Au(SbF_6)_2Au(AuF_4)_2$ with a nearly 4-fold molar excess of $KAuF_4$ dissolved in aHF. Since the former compound is of very low solubility in aHF and slow to solvolyze, the complete replacement of SbF_6 by AuF_4 appeared to be the predominant interaction (see eq 1). The magnetic behavior of the product (see Figure 3) is almost the same as that of $Au(SbF_6)_2Au(AuF_4)_2$ (see Figure 2), and as in that compound, it can be safely concluded that Au(II) centers cannot be joined by a bridging F ligand in common. It is also highly probable that each gold atom [whether Au(II) or Au(III)] will be square-coordinated by F ligands. These considerations, and stoichiometric requirements, lead to the expectation that each $Au^{II}F_4$ shares each of its F ligands with four $Au^{III}F_4$, and each of the latter (on average) shares with two $Au^{II}F_4$. Indeed, if the hexagonal indexing of the $Ag(AgF_4)_2$, $Ag(AuF_4)_2$, and $Au(AuF_4)_2$ diffraction data is correct (Tables SIX, SX, and SXI), the A(II) atoms will probably be located in 2-fold axial-symmetry sites of the hexagonal unit cell ($^1/_2$, 0, z, etc). This would allow a square $A^{II}F_4$ group to share each of its four F ligands with each of four A(III) atoms (in positions x, y, and z). The latter, also in a roughly square F-ligand environment $\{A^{III}F_4\}$ should be linked by two F bridges (probably in *cis* arrangement, as in the trifluorides[9]) to two A(II) atoms. The a_o dimension (∼12.9 Å) is in harmony with either 12-membered rings of alternating A(II) and A(III), bridged by F [i.e., $\{-F-Au^{II}-F-Au^{III}-\}_3$] or by such a 12-atom sequence forming one turn in a helical structure (not unlike segments of the AgF_3 and AuF_3 structures[9]).

Treatment of $Au(AuF_4)_2$ with excess alkali fluoride in aHF destroys all Au(II) according to the equation

$$3Au^{II}\{Au^{III}F_4\}_2 + 8F^- \rightarrow Au + 8Au^{III}F_4^- \quad (3)$$
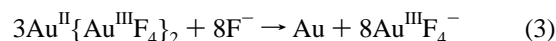
This instability with respect to the metal and the A(III) oxidation state, is not observed in either[9] Ag_3F_8 or AgF_2, the latter withstanding attack[34] by a saturated solution of KF in aHF over many days at 20 °C. These and other differences are attributable to the relativistic effect. Because of the greater binding energy of the valence s electron of gold, the atomization and first ionization enthalpies of gold are higher than for silver. However, from the same cause, the binding energies of the gold-atom d electrons are lowered. The relative ease of formation[5,31] of AuF_4^- and AuF_6^- are testimony to this, as is the high thermodynamic stability of AuF_3 ($\Delta H_f°_{298} = -83$ kcal mol^{-1})[35] which stands in contrast to the thermodynamic instability of AgF_3, which loses fluorine in aHF at room temperature.[9]

AgF_2 does not behave chemically like AuF_2. It does not disproportionate to Ag and $Ag^{II}\{Ag^{III}F_4\}_2$ and, in highly basic aHF, does not give Ag and AgF_4^-. These differences between AgF_2 and AuF_2 must be associated with the higher excitation energy involved in making Ag(III), compared with Au(III), as well as the energy of forming metallic A from A(II). The latter is more favorable for Au than for Ag. A rough measure of this energy is given by the sum of the atomization enthalpy and the first and second ionization potentials for the two elements. The sums are as follows: Ag, 738.3; Au, 773.6 kcal mol^{-1}. These sums can also give us a rough assessment of the enthalpy of formation of AuF_2, since $\Delta H_f°_{298}$ of AgF_2 is known (-87.3 kcal mol^{-1}).[27] Making the approximation that AgF_2 and AuF_2 are ionic and structurally similar, the differences in their enthalpies of formation equate with differences in the sum quoted above, combined with lattice energy differences. Because of the similarity of the Au(II) and Ag(II) radii in the *xy* plane, it can be expected that the binding together of the A^{2+} and F^- in the puckered sheets of the AgF_2 structure[33] could provide the greatest part of the lattice energy, and this contribution would be the same for both AgF_2 and AuF_2. As has been noted earlier, the d_{z^2} electron pair of Au(II) is ∼8 Å^3 larger in effective volume than that of Ag(II). Separation of the puckered sheets of AuF_2 should therefore be greater than in the AgF_2 case. That part of the lattice energy, which derives from sheet-to-sheet attraction, will consequently be less for AuF_2 than for AgF_2. But the sheet-to-sheet distances, even in AgF_2, are large[33] and indicative of weak binding. Even if the lattice energies were the same, the sum of the atomization and first two ionization enthalpies favors AgF_2 over AuF_2 by 35.3 kcal mol^{-1}. We can expect the impact of lattice energy[36] to increase this preference for AgF_2, but probably by not more than another 40 kcal mol^{-1}. Therefore the estimated $\Delta H°_{298}$ of disproportionation ($3AuF_2 \rightarrow Au + 2AuF_3$) ranges from -10 kcal mol^{-1} [with no difference in the AgF_2 and AuF_2 lattice energies (U)] to -130 kcal mol^{-1} [with $U(AgF_2) - U(AuF_2) = -40$ kcal mol^{-1}]. The change in entropy[37] for the disproportionation should be close to 0. Thermodynamic instability of AuF_2 with respect to metallic gold

(33) Jesih, A.; Žemva, B.; Bachmann, B.; Becker, St.; Müller, B. G.; Hoppe, R. *Z. Anorg. Allg. Chem.* **1990**, *588*, 77.

(34) AgF₂ showed no sign of interaction with a KF/HF mixture of ∼20:1 molar ratio over 5 days at ∼20 °C. Dr. M. Whalen, U.C. Berkeley, unpublished observation.

(35) Woolf, A. A. *J. Chem. Soc.* **1954**, 4694.

(36) The Madelung part of the lattice energy is inversely proportional to the sum of the ionic radii. The latter can be roughly approximated[37] by the cube root of the effective formula unit volume (FUV). FUV(AgF₂) (see ref 33) is 42 Å³. Assuming FUV(AuF₂) to be 8 Å³ greater, the lattice energy of AuF₂ would be 0.944 times the lattice energy (U) of AgF₂. From the Born−Haber cycle, the latter is −701 kcal mol⁻¹; therefore U(AuF₂) would be ∼−661 kcal mol⁻¹.

(37) Thrasher, J. S., Strauss, S. H., Eds. *Inorganic Fluorine Chemistry: Toward the 21st Century*; ACS Symposium Series, 555; American Chemical Society: Washington, DC, 1994; Chapter 2.

and AuF_3 is therefore indicated. But Au(III) must be energetically more favorably placed when in an anion $(AuF_4)^-$, and this may be why the solvolysis of $Au(SbF_6)_2$ by aHF produces gold with $Au^{II}\{Au^{III}F_4\}_2$ and not with AuF_3.

Supporting Information Available: Listings of crystal data, interatomic distances, angles, and thermal parameters (14 pages). See any current masthead page for ordering and Internet access instructions.

JA9630654